Climate change and deforestation drive the displacement and contraction of tropical montane cloud forests

Santiago Ramírez-Barahona (santiago.ramirez@ib.unam.mx)
Universidad Nacional Autónoma de México https://orcid.org/0000-0003-3999-6952
Ángela P. Cuervo-Robayo
CONABIO https://orcid.org/0000-0002-8490-4095
Kenneth Feeley
University of Miami https://orcid.org/0000-0002-3618-1144
Andrés Ortiz-Rodríguez
Universidad Nacional Autónoma de México
Antonio Vásquez-Aguilar
Instituto de Ecología AC
Juan Francisco Ornelas
Instituto de Ecologia, AC
Hernando Rodríquez-Correa
Universidad Nacional Autónoma de México

Biological Sciences - Article

Keywords: climate change, forests, cloud forests, deforestation

Posted Date: December 2nd, 2021

DOI: https://doi.org/10.21203/rs.3.rs-1036888/v1

Climate change and deforestation drive the displacement and contraction of tropical montane cloud forests

Santiago Ramírez-Barahona[1,*], Angela P. Cuervo-Robayo[2], Kenneth Feeley[3], Andrés Ernesto Ortiz-Rodríguez[1], Antonio Acini Vásquez-Aguilar[4], Juan Francisco Ornelas[4], Hernando Rodríguez-Correa[5]

[1] Departamento de Botánica, Instituto de Biología, Universidad Nacional Autónoma de México (UNAM), Circuito Exterior s/n, Ciudad de México, 04510, Mexico.

[2] Comisión Nacional para el Conocimiento y Uso de la Biodiversidad (CONABIO), Insurgentes Sur-Periférico, Tlalpan, Ciudad de México, 14010, Mexico.

[3] Department of Biology, University of Miami, Coral Gables, FL, 33146 USA

[4] Departamento de Biología Evolutiva, Instituto de Ecologia, AC (INECOL), Carretera antigua a Coatepec No. 351, El Haya, Xalapa, Veracruz, 91073, Mexico.

[5] Escuela Nacional de Estudios Superiores Unidad Morelia, Universidad Nacional Autónoma de México (UNAM), Antigua Carretera a Pátzcuaro 8701 Ex Hacienda de San José de la Huerta, Morelia, Michoacán, 58190, Mexico

* Author for correspondence:

Santiago Ramírez-Barahona

email: santiago.ramirez@ib.unam.mx

Global climate change and habitat loss are displacing tropical montane forests along mountain slopes[1–4]. Cloud forests are one of the most diverse and fragile of these montane ecosystems[5–8], yet little is known about the historical and ongoing impacts of anthropogenic disturbances on these forests. Here we assess historical (1901–2016) changes in the altitudinal range of vascular plant species in Mesoamerican cloud forests and evaluate the relative impacts of climate change and land-use alterations. By analysing thousands of occurrence records from public biological collections, we uncovered common altitudinal shifts across species and suggest an overall contraction of cloud forests starting in the late 1970s. We infered a pervasive and interrelated impact of rising temperatures, changing precipitation patterns, and deforestation on the distribution of cloud forest species across Mesoamerica. Over the last fifty years, cloud forests have declined due to deforestation and warmer and more (seasonally) arid climates[9–11]. This is pushing species' to contract their altitudinal ranges and may lead to an increasing probability of abrupt and devastating declines of population sizes, local adaptation, and migration.

Anthropogenic climate change is altering species ranges and abundances[1,2] and in some cases, is creating phenological mismatches and population declines across ecosystems[12–16]. Indeed, recent evidence suggests that many tropical communities have experienced significant changes in species composition and geographic range shifts in response to climate change over the last fifty years[3,4,17–23]. Global mean surface temperatures have increased by approximately 0.85°C over the past 130 years. Two distinct periods of warming have occurred during these years, 1910–1945 and from 1970 onwards[24], with the later being characterized by a steep increase in mean temperatures[10]. Changes in precipitation are much less consistent but rainfall has generally decreased in the tropics[24], which combined with increasing temperatures and vapor pressure deficit may lead to increasing water stress for many organisms.

In theory, species can respond to these rapid changes in climate through *in situ* acclimation[25], adaptation of populations to changing conditions[13,25], or migration of populations through habitat tracking (that is, range displacement)[2,13,16,25]. In the tropics, species migrations will be primarily towards higher elevations due to a shallow latitudinal temperature gradient[25–27]. Recent upslope shifts of species have been recorded across tropical mountains[3,4], yet evidence also suggests that some species have not shifted their ranges or have undergone downslope shifts[23]. These idiosyncratic responses of species to climate change can be partially attributed to spatial (and temporal) variability of climate change and its relationship with the biological and ecological attributes of different species[28]. For example, the range of some species may be determined primarily by temperatures, whereas the range of others may be determined more by water availability, soil characteristics, or competition. Therefore, although downslope shifts run counter to the general expectations of global warming[16,25], they may be explained by local/regional alterations to rainfall patterns[29], biological interactions (*e.g.*, predation, competition)[30], life history traits[25], or to other anthropogenic pressures such as land-use change[31,32].

Altitudinal shifts have already led to changes in species composition in many tropical forests, including the emergence of novel communities and the increase in the relative abundance of lowland, warm-adapted species in mid to high altitude montane forest communities[17,33]. If species fail to adequately respond to climate change, or their response is hindered by land-use changes[30] or changing community structure, local extinction of populations will likely increase[1,13,25]. Neotropical montane cloud forests are one of the most biodiverse ecosystems in the world and are highly vulnerable to climate alterations[5–8]. In Mesoamerica alone, these forests harbour more than 6,500 plant species[34] in less than 1% of the region's terrestrial surface. Today, less than 20% of the region's cloud forests are under protection, but this has not halted human disturbance on the few remaining and protected cloud forests[35]. Historical climate data shows a rapidly changing climate across the geographic range of cloud forests[11], which agrees with the

global trend of accelerated change since the 1970s[10]. In addition, historic land-use change suggest that human encroachment has led to more than half of the original forest cover (that is, pre-industrial) being lost to deforestation[7,35]. Disentangling the relative impacts of climate change and land-use changes on the range dynamics of cloud forest species remains a major challenge and a top conservation priority.

Climate change may represent a great threat to cloud forests[8] and, in synergy with unrelenting rates of deforestation, could exacerbate their critical state [7,35,36]. A first step to address cloud forests' vulnerability to anthropogenic disturbances is to assess changes in their distribution, and that of their constituent species, over the recent past. However, the extent to which climate change and other anthropogenic activities have impacted Mesoamerican cloud forest communities over the last century remains poorly explored. Here we address this critical knowledge gap by analyzing data from biological collections with temporal and spatial metadata containing invaluable information on the historical range dynamics of species[19]. We combine these data with historical yearly data for climate and land-use, and information on species' growth forms to assess whether cloud forest species have undergone altitudinal shifts over the last century.

Results and Discussion

We assessed the changes in the altitudinal ranges of 419 cloud forest plant species over the period 1901–2016 by using historical occurrence data. Our analyses revealed a general trend of altitudinal shifts and range contractions in cloud forest plant species (**figure 1**). The altitudinal shifts inferred through simulation show an inflection point in range dynamics among cloud forest species over the last fifty years, starting around the 1970–1980s. The observed shifts coincide, albeit with a clear time lag, with the onset of an the documented acceleration in the pace of climate and land-use occurring since the 1970s[10,37]. Our results suggest opposite shifts in the upper and lower species' range limits (**figure 1a,c**), which support a general contraction of species' elevation ranges (**figure 1d**).

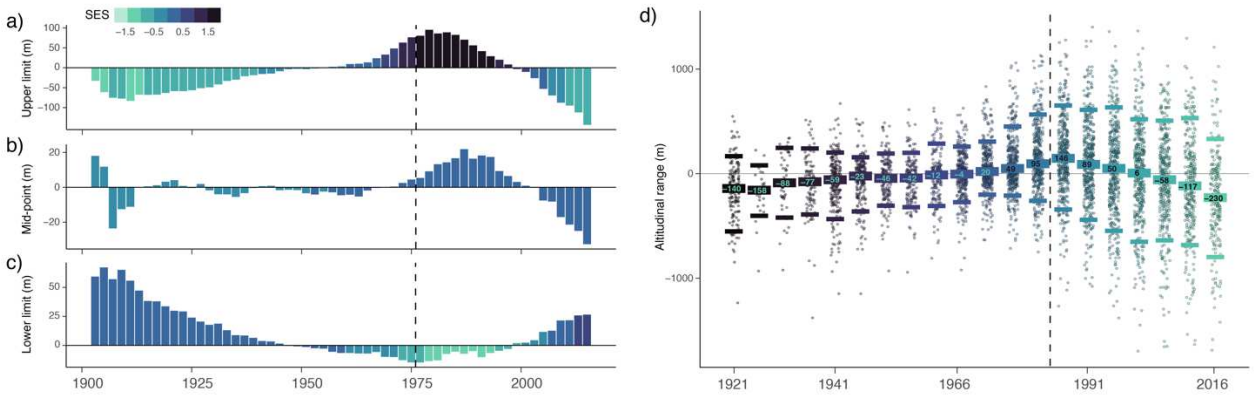

Figure 1. Historical altitudinal ranges for vascular plant species across Mesoamerican cloud forests over the period 1901–2016. a–c, mean deviations from baseline estimates (that is, species' averages during 1901–1975) for the (a) upper limit, (b) mid-point, and (c) lower limit of species' ranges. Values are based on the predicted values of the fitted smoothing splines. d, observed altitudinal ranges (deviations from baseline estimates) over the period 1921–2016 using the time-bins employed for the Piecewise Growth Model (PGM). Crossbars indicate the first and third quantiles (upper and lower crossbars, respectively), and the median (middle crossbar); numbers in the middle crossbar depict the values for the median for each period. Colour scale in a–c represents the mean Standardized Effect sizes (SES) across species estimated through simulations. Vertical dashed lines in a–d indicate the pre-definend breakpoint (that is, 1975–1976).

However, we observed some differences among species in the direction of altitudinal range shifts (upslope or downslope). At least some of these discrepancies appear to be associated with differences in the elevations where the species occur (that is, their mean altitude prior to 1976) and differences in species' growth forms (**supplementary figure S1–S3**). Even when considering species with no positive evidence of elevational shifts, we observe that the average altitudinal trends agree with a general response of cloud forests to anthropogenic influences. These trends could translate into a general historical tendency of elevational range contractions of cloud forests and a decreased capacity for species' migrations[35].

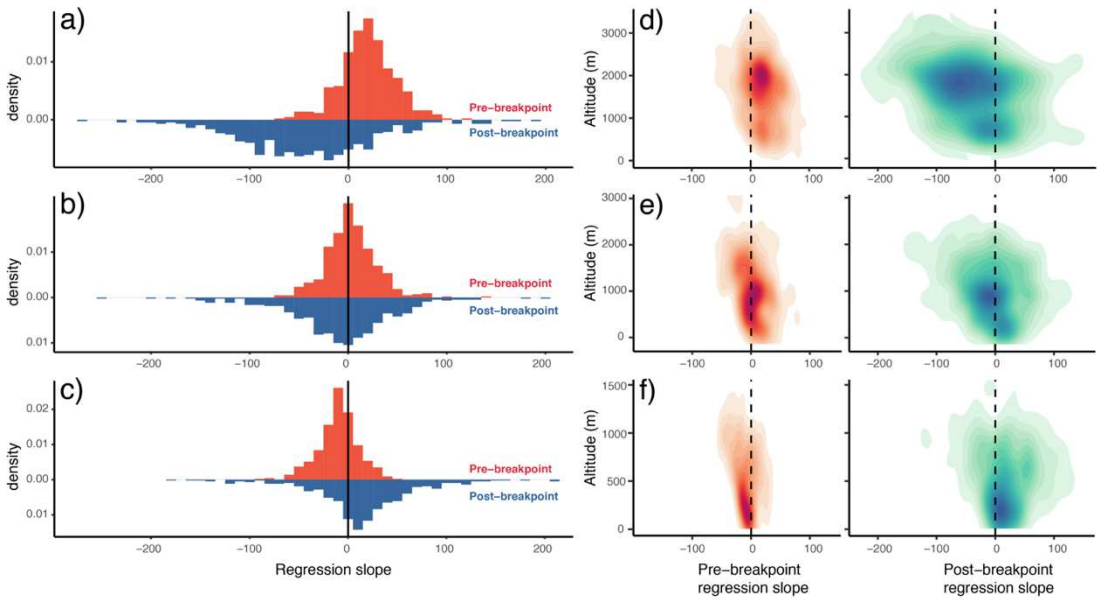

Figure 2. Historical altitudinal trends for vascular plant species across Mesoamerican cloud forests over the period 1901–2016. a–c, histograms showing the distribution of the per-species slopes for the (a) upper range limit, (b) range mid-point, and (c) lower range limit, estimated using a Piecewise Growth Model with two time periods: 1901–1975 (pre-breakpoint) and 1976–2016 (post-breakpoint). d–f, two-dimensional density plots showing the distribution the pre- and post-breakpoint slopes as a function of species' mean elevations. Darker colours indicate a higher density of slopes falling within the corresponding regions. Model coefficients for the Piecewise Growth Models are shown in Supplementary tables S1–S3.

Species' responses have been temporally and spatially heterogeneous across the region, highlighting specific periods with marked shifts across altitudinal belts[38,39]. To test for time-varying changes in the altitudinal ranges of cloud forest species, we fitted a Piecewise Growth Model to estimate species' altitudinal trends before and after a pre-defined year. Based on previous evidence of historical climate and land-use changes[10,37], we defined this breakpoint in the mid-1970s (that is, 1975–1976) and found clear differences between pre- and post-breakpoint trends for the lower and upper range limits (**figure 2**). For both the range limits, pre- and post-breakpoint trends show opposite signs and non-overlapping confidence intervals (**figure 2a,c; supplementary table S1–S3**). In contrast, the altitudinal mid-points of species ranges show less-marked differences between the

150 time periods (**figure 2b**), and in this case a slope of zero (that is, no altitudinal
151 shift) can explain the observed pre-breakpoint trends (**supplementary table S2**).
152 Importantly, there is no indication of an effect of elevation on the observed
153 differences between pre- and post-breakpoint trends, suggesting that most species
154 exhibit the same patterns irrespective of differences in their elevational
155 preferences.

156 The results of the Piecewise Growth Model and the simulations suggest that
157 the upper range limit and, to a lesser extent, the mid-point of species' ranges
158 underwent significant shifts after the 1970s (**figures 1,2**), with post-breakpoint
159 downslope trends (**supplementary table S1,S2**) that are reflected in significantly
160 lower altitudes with respect to baseline means. Importantly, this shift to a
161 downslope trend was accompanied by a parallel upslope shift in species' lower
162 range limits (**figures 1c,2c; supplementary table S3**). These patterns are
163 consistent with climate change during the last century (**figure 3**), which is
164 ubiquitous across Mesoamerica and Mesoamerican cloud forests but temporally
165 and spatially heterogeneous[11]. In particular, we observed substantial deviations
166 from baseline temperature and precipitation (that is, the mean climatologies during
167 1901–1975) that have accelerated since the 1970s (**figure 3**). This is consistent
168 with previous reports of the temporal and geographic trends of changing
169 temperature and precipitation across Mesoamerica[11], showing a dramatic increase
170 of mean annual temperature over the last fifty years[9–11].

171 In general, the historical climate data (**figure 3a,b**) support previous
172 evidence that climate change is causing montane regions of Mesoamerica to
173 become warmer and more (seasonally) arid[33]. These spatially heterogenous
174 changes in climate may increase the vulnerability of cloud forests since species will
175 not be able to track the shifts in suitable climates through just upslope
176 migrations[13,25,30]. In this context, the uneven changes in temperature and
177 precipitation we see across altitudinal belts can partly explain the observed shifts
178 and contraction in species' ranges. Changes to temperature and precipitation

seasonality have been most pronounced at both the lower (< 1,000 m) and upper elevations (> 2,500 m) of cloud forest distributions (**figure 3**). As with temperature, precipitation regimes have changed over the same time period (**figure 3c,d**), with increasingly wetter conditions through time (**figure 3d**); however, this increase in precipitation appears to be accompanied by stronger precipitation seasonality (**figure 3c**). The increase in precipitation seasonality may be of particular concern for cloud forest plant species, because many are highly sensitive to seasonal fluctuations in humidity levels and water stress[35,36,40].

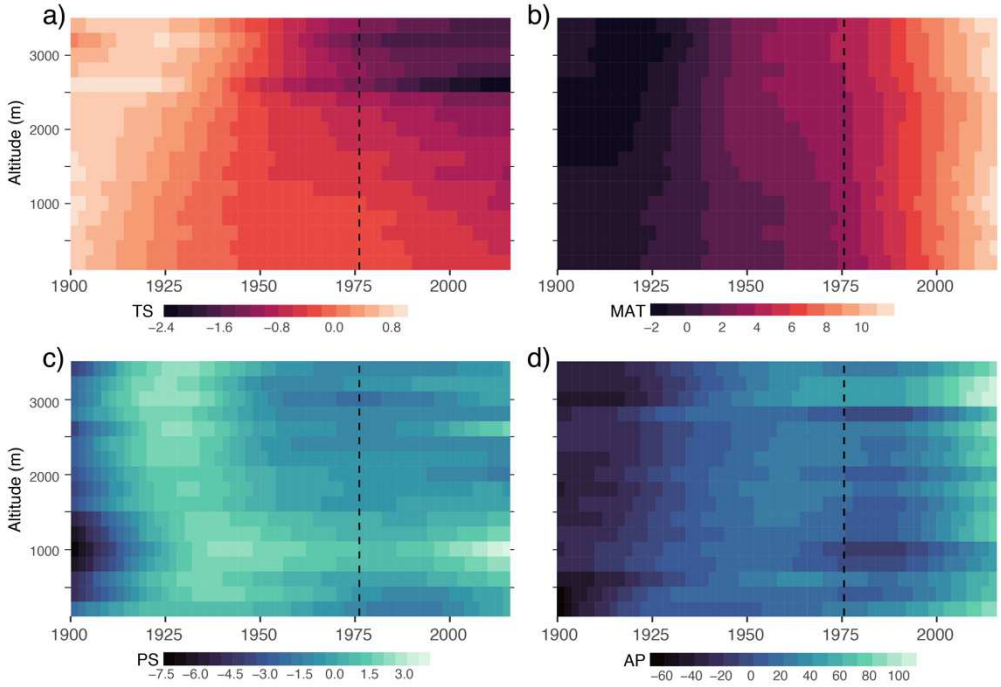

Figure 3. Historical changes in temperature and precipitation across Mesoamerican cloud forests localities over the period 1901–2015. a–d, bi-yearly deviations from baseline averages (1901–1975) in (a) temperature seasonality, (b) mean annual temperature, (c) precipitation seasonality, and (d) annual precipitation; darker colours indicate below-average conditions an brighter colours above-average conditions. Climate data is based on the CHELSAcruts high resolution temperature and precipitation time series for the 20th century[61]. Vertical dashed lines in a–d indicate the pre-definend breakpoint (that is, 1975–1976).

A high proportion of primary cloud forest localities have been historically subjected to human disturbance, which is indicative of land-use changes affecting

cloud forests throughout the region[31]. Assuming that most of the focal species are preferentially found within primary forests, or in areas with moderate to low levels of disturbance[35,41], the heterogeneity in land-use changes across altitudinal belts could have had a profound impact on their distributions, and hence the distribution of cloud forests, through time. We found substantial changes in the extent of primary forest cover over the period 1901–2015 (**figure 4**). Based on the historical land-use data we estimated that by 1936, ~44% (~38–59% across altitudinal belts) of the cloud forest localities in our dataset corresponded to primary forest, but by 2015 only ~11% (~8–14% across altitudinal belts) of these localities remained as primary forest. However, the loss of primary forest cover has not been constant over time and a dramatic decline of 35.2% of the original forest cover (that is, classified as primary forest by 1936) is observed over the period 1976–1996.

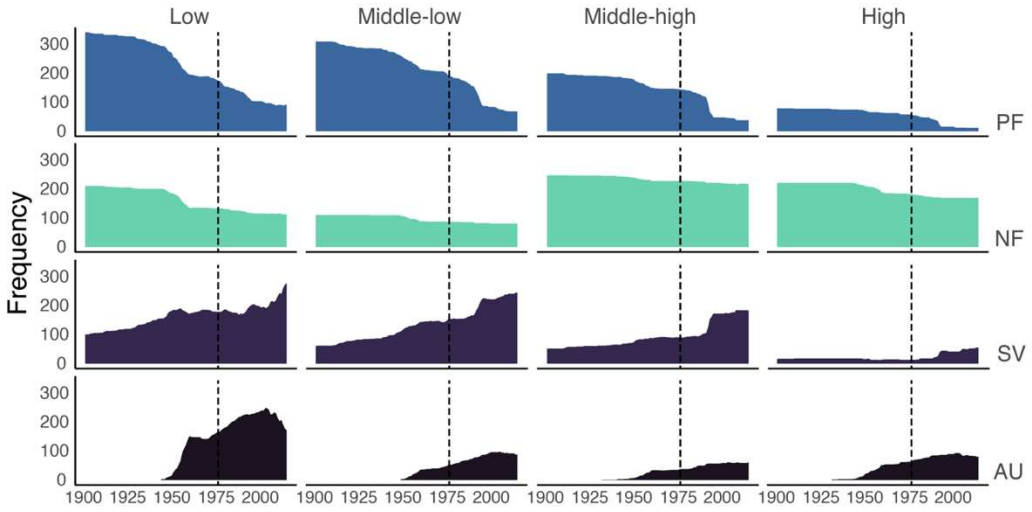

Figure 4. Historical trends in land-use across Mesoamerican cloud forests localities over the period 1901–2015. Area plots showing the proportional area occupied by the four land-use land-cover (LULC) categories: Agriculture-urban (AU), Primary forests (PF), Non-forest vegetation (NF), and Secondary vegetation (VG). The proportion of each land-use category was estimated across four altitudinal belts: Low (0-300 m), Middle-low (300–1,000 m), Middle-high (1,000–2,000), and High (>2,000 m). The vertical dashes lines marks the year 1976. Vertical dashed lines indicate the pre-defined breakpoint (that is, 1975–1976).

Despite some uncertainty in the land-use data[37], our results support the well-documented trend of increasing agricultural, urban, and secondary vegetation land-use[31] at the expense of primary forests and non-forest vegetation across altitudinal belts (**figure 4**). One possible scenario is that the lower and upper range limits of species are shifting not only because of warming and aridification, but also as a result of high extirpation rates (that is, local extinction) of populations. There is no indication that proportional land-use change has been more pronounced either at the lowlands or highlands (**supplementary figure S4**). However, primary forests have been historically more abundant at mid-elevations, so proportionally similar losses across altitudinal belts would lead to more pronounced declines in absolute forest cover at both ends of the altitudinal range of cloud forests.

We acknowledge that some of the observed patterns may be attributable to biases inherent to data from biological collections, particularly the concentration of collection effort in particular areas and through time[42]. As such, some of the observed trends may be reflecting a 'false' signal and a shifting sampling bias rather than species responses to climate change or land-use changes. However, simulations designed to account for collector bias indicate that most of the observed trends are at least in part due to actual shifts in the species' altitudinal ranges. That said, there is still the possibility that the observed patterns are being influenced, by geographically heterogeneous rates of deforestation constraining the areas where species can be collected and lead to apparent shifts of species' ranges.

To test for the possible causal influence of both climate and land-use changes on the observed species range shifts, we used a definition of causality that is based on predictability[43,44]. For each species, we calculated multivariate Granger Causality Indices (GCI) and found that overall historical climate and land-use changes –specifically the loss of primary forests and non-forested vegetation– improves the predictions of species' altitudinal shifts through time (**figure 5**). This means that a significant amount of variance in species altitudinal trends can be

explained either by climate change, land-use transformation, or both (**figure 5**). A substantial proportion of species showed significant GCI, supporting a strong causal influence (predictability) of climate change, land-use transformation, and the interaction between the two, on the observed species' altitudinal range shifts (**figure 5**). These causal influence on species altitudinal ranges appears to be ubiquitous across species with different growth forms (**supplementary figure S5–S7**). Although we observed slightly higher GCI estimates for woody species (that is, trees and shrubs) than for herbaceous species, these results support an overarching influence of climate change and land-use transformation across a broad spectrum of cloud forest species.

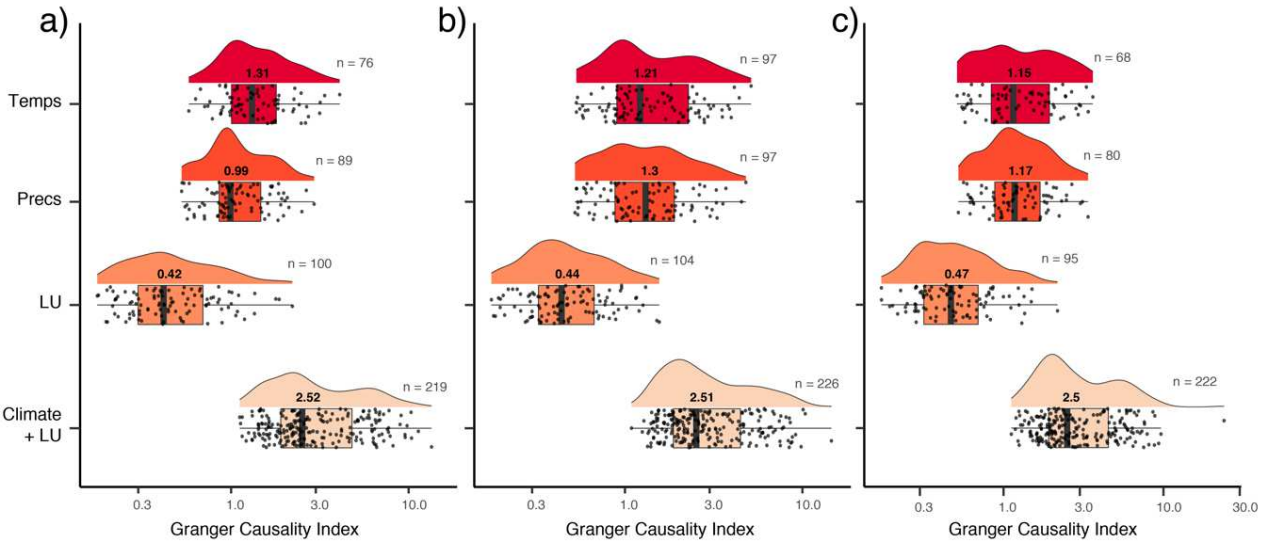

Figure 5. Granger causal influence of climate and land-use change time series on species historical altitudinal trends. a–c, raincloud plots showing the distribution of the per-species Granger Causality Index (GCI) of the different climate change land-use time series for (a) upper range limit, (b) range mid-point, and (c) lower range limit. Numbers within the density plots indicate the median value across species and numbers to the left indicate the number species with a significant GCI (p-value < 0.05).

The inferred synchronous response of species might imply that cloud forests likely respond as cohesive communities, perhaps because the high climatic sensitivity of most species. However, we observe that species' range contractions have increasingly become more variable over the last fifty years, compared to the

inferred responses prior to the 1970s (**figure 1d**). Thus, the impacts of an accelerated environmental degradation of cloud forests could have devastating effects in the near future, affecting community composition, local forest structure, levels of biodiversity, and hydrological cycles[26,40,45,46]. Improving our knowledge of past range shifts on tropical montane ecosystems is imperative if we hope to prevent these valuable ecosystems and species from vanishing in the near future. Our study provides strong evidence for the dire status of cloud forests across the region[6,7,35,36]. Species are being forced into contracting mid-elevational refugia of remaining forest cover, with an overall reduction in their elevational ranges over time. This likely translates into a geographic/altitudinal decline in cloud forest species abundances and may be due to the incapacity for acclimation and *in situ* adaptation, limited dispersal potential, or alteration to forest structure due to canopy thinning and border effects[47]. In light of the temporal dynamics we uncovered, we suggest a breach of a 'climate horizon'[46] – enhanced by land-use changes – beyond which there would be a dramatic increase in the probability of abrupt and devastating disruptions of cloud forest communities.

References

1. Thomas, C. D. *et al.* Extinction risk from climate change. *Nature* **427**, 145–148 (2004).
2. Parmesan, C. & Yohe, G. A globally coherent fingerprint of climate change. *Nature* **421**, 37–42 (2003).
3. Neate-Clegg, M. H. C., Jones, S. E. I., Burdekin, O., Jocque, M. & Şekercioğlu, Ç. H. Elevational changes in the avian community of a Mesoamerican cloud forest park. *Biotropica* **50**, 805–815 (2018).
4. Grabherr, G., Gottfried, M. & Pauli, H. Climate effects on mountain plants. *Nature* **369**, 448 (1994).
5. Rojas-Soto, O. R., Sosa, V. & Ornelas, J. F. Forecasting cloud forest in eastern and southern Mexico: Conservation insights under future climate change scenarios. *Biodivers. Conserv.* **21**, 2671–2690 (2012).
6. Ponce-Reyes, R. *et al.* Vulnerability of cloud forest reserves in Mexico to climate change. *Nat. Clim. Chang.* **2**, 448–452 (2012).
7. Karger, D. N., Kessler, M., Lehnert, M. & Jetz, W. Limited protection and ongoing loss of tropical cloud forest biodiversity and ecosystems worldwide worldwide. *Nat. Ecol. Evol.* **5**, 854–862 (2020).

8. Gardner, T. A. *et al.* The future of hyperdiverse tropical ecosystems. *Nature* **559**, 517–559 (2018).
9. Rahmstorf, S. *et al.* Recent Climate Observations Compared Compared to Projections. *Science (80-.).* **316**, 2007 (2007).
10. IPCC. *Climate Change 2021: The Physical Science Basis. Contribution of Working Group I to the Sixth Assessment Report of the Intergovernmental Panel on Climate Change*. (Cambridge University Press, 2021).
11. Cuervo-robayo, A. *et al.* One hundred years of climate change in. *PLoS Genet.* **15**, e0209808 (2020).
12. Feeley, K. J., Hurtado, J., Saatchi, S., Silman, M. R. & Clark, D. B. Compositional shifts in costa rican forests due to climate-driven species migrations. *Glob. Chang. Biol.* **19**, 3472–3480 (2013).
13. Feeley, K. J., Rehm, E. M. & Machovina, B. perspective: The responses of tropical forest species to global climate change: acclimate, adapt, migrate, or go extinct? *Front. Biogeogr.* **4**, F5FBG12621 (2012).
14. Jezkova, T. & Wiens, J. Rates of change in climatic niches in plant and animal populations are much slower than projected climate change. *Proc. R. Soc. B* **283**, 20162104 (2016).
15. Román-Palacios, C. & Wiens, J. J. Recent responses to climate change reveal the drivers of species extinction and survival. *Proc. Natl. Acad. Sci. U. S. A.* **117**, 4211–4217 (2020).
16. Walther, G.-R. *et al.* Ecological responses to recent climate change. *Nature* **416**, 389–395 (2002).
17. Fadrique, B. *et al.* Widespread but heterogeneous responses of Andean forests to climate change. *Nature* **564**, 207–212 (2018).
18. Chen, I. C. *et al.* Elevation increases in moth assemblages over 42 years on a tropical mountain. *Proc. Natl. Acad. Sci. U. S. A.* **106**, 1479–1483 (2009).
19. Peterson, A. T. *et al.* Twentieth century turnover of Mexican endemic avifaunas : Landscape change versus climate drivers. *Sci. Adv.* **1**, e1400071 (2015).
20. García, D. J.-, Lira-, X. L. A. & Peterson, A. T. Upward shifts in elevational limits of forest and grassland for Mexican volcanoes over three decades. *Biotropica* **53**, 798–807 (2021).
21. Wang, L. *et al.* The earliest fossil bamboos of China (middle Miocene, Yunnan) and their biogeographical importance. *Rev. Palaeobot. Palynol.* **197**, 253–265 (2013).
22. McCain, C. M. & Garfinkel, C. F. Climate change and elevational range shifts in insects. *Curr. Opin. Insect Sci.* **47**, 111–118 (2021).
23. Zu, K. *et al.* Upward shift and elevational range contractions of subtropical mountain plants in response to climate change. *Sci. Total Environ.* **783**, 146896 (2021).
24. Stocker, T. F. *et al. Climate change 2013 the physical science basis: Working Group I contribution to the fifth assessment report of the intergovernmental panel on climate change*. *Climate Change 2013 the Physical Science Basis: Working Group I Contribution to the Fifth*

Assessment Report of the Intergovernmental Panel on Climate Change (2013). doi:10.1017/CBO9781107415324
25. Corlett, R. T. Impacts of warming on tropical lowland rainforests. *Trends Ecol. Evol.* **26**, 609–616 (2011).
26. Foster, P. The potential negative impacts of global climate change on tropical montane cloud forests. *Earth-Science Rev.* **55**, 73–106 (2001).
27. Still, C. J., Foster, P. N. & Schneider, S. H. Simulating the effects of climate change on tropical montane cloud forests (Still, Foster {\&} Schneider, 1999).pdf. **398**, 15–17 (1999).
28. Lenoir, J. & Svenning, J. Climate-related range shifts – a global multidimensional synthesis and new research directions. *Ecography (Cop.).* **38**, 15–28 (2015).
29. Ordonez, A., Williams, J. W. & Svenning, J. Mapping climatic mechanisms likely to favour the emergence of novel communities. **6**, (2016).
30. Rehm, E. M. & Feeley, K. J. The inability of tropical cloud forest species to invade grasslands above treeline during climate change: Potential explanations and consequences. *Ecography (Cop.).* **38**, 1167–1175 (2015).
31. Navarro Cerrillo, R. M., Esteves Vieira, D. J., Ochoa-Gaona, S., de Jong, B. H. J. & del Mar Delgado Serrano, M. Land cover changes and fragmentation in mountain neotropical ecosystems of Oaxaca, Mexico under community forest management. *J. For. Res.* **30**, 143–155 (2019).
32. Ramírez-Barahona, S. & Luna-Vega, I. Geographic Differentiation of Tree Ferns (Cyatheales) in Tropical America. *Am. Fern J.* **105**, (2015).
33. Feeley, K. J., Bravo-Avila, C., Fadrique, B., Perez, T. M. & Zuleta, D. Climate-driven changes in the composition of New World plant communities. *Nat. Clim. Chang.* **10**, 965–970 (2020).
34. Gual-Díaz, M. & Rendón-Correa, A. *Bosques Mesófilos de Montaña de México: Diversidad, ecología y manejo*. *Comisión Nacional para el Conocimiento y Uso de la Biodiversidad* (CONABIO, 2014). doi:10.1007/s10668-016-9830-7
35. Toledo-Aceves, T., Meave, J. A., González-Espinosa, M. & Ramírez-Marcial, N. Tropical montane cloud forests: Current threats and opportunities for their conservation and sustainable management in Mexico. *J. Environ. Manage.* **92**, 974–981 (2011).
36. Bruijzeel, L. A. & Hamilton, L. S. Decision time for Cloud Forests. *IHP Humid Trop. Program.* **13**, 44 (2000).
37. Hurtt, G. C. *et al.* Harmonization of global land use change and management for the period 850 – 2100 (LUH2) for CMIP6. *Geosci. Model Dev.* **13**, 5425–5464 (2020).
38. Gottfried, M. *et al.* Continent-wide response of mountain vegetation to climate change. *Nat. Clim. Chang.* **2**, 111–115 (2012).
39. Chen, I. C., Hill, J. K., Ohlemüller, R., Roy, D. B. & Thomas, C. D. Rapid range shifts of species associated with high levels of climate warming. *Science (80-.).* **333**, 1024–1026 (2011).
40. Bruijnzeel, L. A., Scatena, F. N. & Hamilton, L. S. *Tropical montane cloud*

forests: Science for conservation and management. *Tropical Montane Cloud Forests: Science for Conservation and Management* (Cambridge University Press, 2011). doi:10.1017/CBO9780511778384
41. Gotsch, S. G., Dawson, T. E. & Draguljić, D. Variation in the resilience of cloud forest vascular epiphytes to severe drought. *New Phytol.* **219**, 900–913 (2018).
42. Meyer, C., Weigelt, P. & Kreft, H. Multidimensional biases, gaps and uncertainties in global plant occurrence information. *Ecol. Lett.* **19**, 992–1006 (2016).
43. Damos, P. Using multivariate cross correlations , Granger causality and graphical models to quantify spatiotemporal synchronization and causality between pest populations. *BMC Ecol.* **16**, 33 (2016).
44. Wiener, N. The theory of prediction. in *Modern Mathematics for Engineers* (ed. Beckenback, E. F.) (McGraw-Hill, 1956).
45. Helmer, E. H. *et al.* Neotropical cloud forests and paramo to contract and dry from declines in cloud immersion and frost. *PLoS One* **14**, e0213155 (2019).
46. Trisos, C. H., Merow, C. & Pigot, A. L. The projected timing of abrupt ecological disruption from climate change. *Nature* **580**, (2020).
47. Betts, M. G. *et al.* Global forest loss disproportionately erodes biodiversity in intact landscapes. *Nat. Publ. Gr.* **547**, 441–444 (2017).

Methods

Species occurrence data. We obtained a list of vascular plants for cloud forests from ref.[48]. This is the most comprehensive and well-curated species list and comprises 6,778 plant species that have been recorded in Mesoamerican cloud forests. Prior to processing, we harmonized family and species names using Kew's Plants of the World database[49] and obtained a list of 6,495 species belonging to 221 families of angiosperms, gymnosperms, ferns, and lycophytes.

We used historical distribution data available from the Global Biodiversity Information Facility (GBIF), querying all records under 'Tracheophyta' and considering only 'Preserved Specimens' in our search; this database consisted of 68,570,538 occurrence records[50]. The occurrence records were taxonomically harmonized and cleaned following the procedures described in refs.[51–53]. Briefly,

we first discarded records without species identification and with missing or badly formatted GPS coordinates. Then, we harmonized family and species names using Kew's Plants of the World database[49], which allowed us to match the occurrence database with the list of cloud forest species obtained above.

We used the *CoordinateCleaner* package[54] in R[55] to flag suspect occurrence records meeting one (or more) of the following criteria: (1) equal latitude and longitude, (2) zero latitude and longitude, (3) coordinates falling within a five-kilometre radius of a country's political centroid, (4) coordinates falling within a ten-kilometre radius of a country's capital, (5) coordinates falling within a two-kilometre radius of biodiversity institutions, and (6) coordinates falling in the open ocean using a reference landmass buffered by one degree from the coastline to avoid eliminating species living on the coast. In addition, for each species we applied the geographic outlier test to flag suspect records. This test estimates pairwise geographic distances among all records of a species and then flags those records with a minimum distance to all other records greater than a defined threshold, in this case 300 km; flagged records represent single occurrences isolated from the rest of the known distribution of the species. Lastly, we flagged additional suspect records using the geographic information available in Kew's Plants of the World database[49] that scores the 'native' or 'non-native' status of species across the world using the World Geographic Scheme for Recording Plant Distributions[56].

Since we aimed to address the historical dynamics of cloud forests in Mesoamerica, we discarded species with occurrence records located outside the American continent (longitudinal limits, 30º–135ºW). Furthermore, the floristic list includes species that are widespread and not restricted to cloud forests (or other montane forest communities). To further identify these species, we used the data on terrestrial eco-regions of the world to assign every occurrence record to one of 14 recognized biomes[57]. For each species, we estimated the proportion of records within each biome and discarded species with more than 2.5% of their occurrences

459 within any of the following biomes: tropical dry forests, temperate grasslands,
460 flooded grasslands, tundra, Mediterranean forests, deserts and xeric scrubland,
461 and mangroves. We considered the frequent presence of species within these
462 biomes as indicative of taxonomic problems in the original species list (that is,
463 erroneous species determinations) or indicative of occurrence records in cloud
464 forests being the result of invasive, non-native, or generalist species.

465 In sum, we obtained a database comprising 74,701 occurrence records for
466 899 cloud forest plant species (14% of the total number of species in ref.[48]), which
467 belong to 148 families of angiosperms (766 species), ferns (114), lycophytes (10),
468 and gymnosperms (9). We used these occurrence records to perform all
469 subsequent analyses. For the main analyses, we limited the study area to
470 comprise grid-cells in Continental America (that is, excluding the Antilles) within
471 12–26ºN, limiting our dataset to 1,895 grid-cells, and we excluded records with
472 dates prior to 1901. We selected species with more than 50 records (419 species,
473 62,973 records). Data processing was handled in R[55].

474 *Plant trait data.* We compiled data on growth form for the target species from a
475 dataset obtained from the TRY Plant Trait Database[58,59]. For consistency, prior to
476 analysis we harmonized species names using Kew's Plants of the World
477 database[49]. Given the heterogeneous categorization of growth forms in the 'raw'
478 TRY dataset, we homogenized and categorized growth-form data into four distinct
479 categories: (i) woody and non-woody climbers; (ii) epiphytes; (iii) herbs; (iv) shrubs;
480 and (v) trees. Several species in the TRY dataset have two or more records and
481 are categorized into two or more growth-form categories. Thus, we decided to
482 score species into a single category following a majority rule consensus. Although
483 the distinction among categories is not clear-cut, our scheme is aimed at
484 distinguishing among broad growth-form categories and habitats among cloud
485 forest species. Data processing was handled in R[55].

486 *Land-use series.* We obtained land use and vegetation data for the region from
487 ref.[60], who selected and transformed the data from the Land Use Harmonization

Project (LUH2)[37]. The LUH2 is a global terrestrial dataset at 0.25º spatial resolution that provides land-use and land-cover (LULC) data from 850 to 2300[37,60]. We used the final dataset provided by ref.[60] and retrieved LULC data for the years 1901–2016. For each of the 1,895 grid-cells (resolution of 0.083º, ~9 km^2) in our occurrence database we extracted yearly data on land-use. The original LULC data includes the following twelve categories[37,60]: forested primary land, non-forested primary land, potentially forested secondary land, potentially non-forested secondary land, managed pasture, rangeland, urban land, C3 annual crops, C3 perennial crops, C4 annual crops, C4 perennial crops, and C3 nitrogen-fixing crops. For our analyses, we summarized these categories into four broad categories: (1) AU, urban and agricultural; (2) NF, non-forested primary vegetation; (3) PF, primary forested vegetation; and (4) SV, secondary vegetation.

We visualized temporal changes across land-use categories using chord diagrams, which represent 'flows' between multiple entities. In this case, the entities represent land-use categories at two distinct time points (for example, PF-1936 and PF-1956) and the flows represent the proportion of grid cells transitioning between categories from past to present (for example, PF-1936 to AU-1956). The size of each category is represented by a fragment of the outer circle, where all the fragments for a given time period sum up to 1. This way we can estimate and visualize the proportional changes through time for any given land-use category and the proportional size of different transitions across categories. We estimated land-use transitions between 1936 and 2015; we chose 1936 as the starting point because the AU category appears first in our grid-cells during the 1930s. Data processing was handled in R[55].

Historical climate change series. We used the climate data from the CHELSAcruts high resolution temperature and precipitation time series for the 20th century[61]. These time series include monthly data for maximum temperature, minimum temperature, and net precipitation at a 30 arc-sec spatial resolution. We extracted climate data for every occurrence record and then aggregated the monthly data

517 into four yearly variables: annual precipitation (Ann_Prec), precipitation seasonality
518 (CV_Prec), mean annual temperature (Mean_temp), and temperature seasonality
519 (CV_temp). Variable processing was handled in R[55]. We extracted climate and
520 elevation data for every occurrence record, which we then aggregated for the
521 1,895 grid-cells comprising our study area.

522 We used the aggregated climate data to visualize climate change series
523 within cloud forest localities, extracting yearly climate data for the period 1901–
524 2016 for each locality. For each climatic variable, we estimated a rolling mean
525 using a moving window of ten time points centred on the corresponding year (that
526 is, the time window for 1955 is 1951–1960), with partial estimates allowed (that is,
527 the time window for 1901 is 1901–1906). We then fitted cubic smoothing splines of
528 climate as a function of time for each locality, using a smoothing parameter that
529 was automatically set between 0.45 and 0.7 to avoid over-fitting; smooth model fit
530 was performed as implemented in the *'npreg'* package[62] in R[55]. We used the
531 resulting smoothing spline models to estimate average 'predicted' climate values
532 every two years. We set 1975–1976 as a breaking point in historical climate trends
533 based on empirical evidence[10] and estimated climate averages before this point
534 (baseline means) across 200-meter altitudinal belts. We then calculated deviations
535 from these baseline estimates across the full climate series for every altitudinal
536 belt, separately. Data processing was handled in R[55].

537 *Historical altitudinal series.* We used the geographic occurrences for the selected
538 species to evaluate altitudinal series for each species for the period 1901–2016.
539 For this, we used the GTOPO30 global digital elevation model (US Geological
540 Service' Earth Resources Observation and Science Center) to assign altitudinal
541 data to every occurrence record; this global elevation model has a grid resolution
542 of 30 arc-seconds (~1 km^2).

543 To characterize shifts in species' altitudinal ranges, we used information on
544 the year of collection of every record to estimate a rolling median of altitude (mid-
545 point) for each species as described above for climate series. We only considered

546 rolling estimates calculated from a minimum of ten occurrence records, which
547 ensures that every rolling estimates is based on an average of one record per year.
548 As described above for climate series, we fitted cubic smoothing splines of mid-
549 point altitude as a function of time for each species; smoothing splines were only
550 fitted for species with at least ten data points (rolling estimates). For each species,
551 we estimated the average 'predicted' altitude every two years since the species'
552 first historical occurrence.

553 We also assessed shifts in the lower and upper limits of species' altitudinal
554 ranges as described above. To minimize the possible influence of outlying records,
555 we used the 0.025 and 0.975 quantiles of the altitudinal range to approximate the
556 lower and upper limits, respectively. Finally, we estimated the breadth of the
557 altitudinal range of species by taking the difference between the rolling estimates
558 for the lower and upper range limits. This allowed us to visualize trends of range
559 contractions/expansions through time.

560 *General altitudinal shifts.* We tested for a general altitudinal shift of cloud forests by
561 fitting a Piecewise Growth Model (PGM) using the '*lme4*' package[63] in R[55]. We
562 fitted PGM to the lower, mid-point, and upper altitude of species separately, using
563 the Nelder-Mead optimizer. To fit the PGM we summarised the altitudinal data into
564 twenty periods (5-year bins); due to the reduced data prior to 1921, we defined the
565 first time period as a 20-year bin (that is, 1901–1921). Briefly, the model estimates
566 the average slope and intercept of the altitudinal series while modelling non-linear
567 change through time. The general fitted PGM takes the form ('*lme4*' syntax),

568 $$y_i \sim intercept + slope_0 + slope_1 + (intercept \mid Species) +$$

569 $$(0 + slope_0 \mid Species) + (0 + slope_1 \mid Species),$$

570 where y_i is the mean altitude across species and $slope_0$ and $slope_1$ represent the
571 slope coefficients before and after a pre-defined breakpoint. This model
572 incorporates random effects for the intercept and the two slopes (that is, species
573 effects) and uncorrelated random effects for $slope_0$ and $slope_1$. We used 1975–

1976 as a breaking point to segment the time series using 'dummy' variables. The PGM was assessed against less complex nested models, that is growth models with a single time trend (that is, a single slope coefficient) and fewer random effects (that is, only random intercepts). We fitted PGM to the lower, mid-point, and upper altitudinal limits of species, separately.

Significance of species' altitudinal series. In order to account for the possibility of collection bias impacting the observed species' altitudinal shifts, we compared the observed series against null models based on time-varying collection efforts. Basically, we implemented a re-sampling approach of the complete occurrence database by generating 'simulated species' that match the per-year sampling intensity and the altitudinal range of species. To achieve this, for a given species, we first estimated the recorded altitudinal range throughout the entire period (that is, 1901–2016) and counted the number of occurrence records per year. We used this information to identify occurrence records (across all species in the database) within the altitudinal range of the focal species, and then sampled this subset of occurrences using the per-year sampling intensity of the focal species. In principle, this procedure generates a sample of records matching the historical altitudinal range and temporal sampling effort for a given species.

For every 'simulated species', we produced rolling estimates, fitted smoothing splines and estimated average 'predicted' values as described above. We constructed 500 replicates of the null models (that is, simulated species) for every species, and compared the empirical values against those obtained through simulation. We estimated the mean and standard deviation across the 500 replicates and estimated per-species Standardized Effect Sizes (SES) at time *i* as:

$$SES_{Ti} = OBS - MEAN / SD,$$

Where *OBS*, *MEAN*, and *SD* correspond to the empirical value, the mean and standard deviation of the null model, respectively. SES_{Ti} indicates whether observed altitudes are higher or lower than expected under the null model; their

significance is approximated using 95% confidence intervals around zero (± 1.96). We constructed the null models in R[55].

We used the Standardized Effect Sizes (SES_{Ti}) for the average 'predicted' altitude over the period 1901–2016 to visualize the overall trend of altitudinal shifts among cloud forest species. For this, we estimated per-year averages of observed altitudes across species, but only for estimates with associated significant SES_{Ti}. We further visualized the overall trends by grouping species into altitudinal and growth-form categories; for altitude, we classified species into four altitudinal belts based on their mean elevation: (i) low (148), (ii) mid-low (164), (iii) mid-high (166), and (iv) high (42).

Influence of climate change and land-use on altitudinal series. Using the species' altitudinal series, we assessed whether species responses are causally influenced by climate and land-use changes. For this, we employed the Granger Causality Index (GCI) that uses a concept of causality based on prediction[43,44]. More specifically, the Granger Causality test is a statistical hypothesis to test whether one (or more) time series is useful for predicting another series. For each species, we summarised climate and land-use series across the grid cells where the target species has been recorded. For the climate series we estimated series for each of the four yearly variables and for the land-use series we estimated the temporal change in the frequency of grid-cells with forested (PF) and non-forested (NF) primary vegetation. Prior to estimating the GCI, we pre-whitened all series according to an ARIMA model fitted to the altitudinal series (that is, the ARIMA model was fitted by selecting the best model according to the AICc value)as implemented in the 'forecast' package[64,65] in R[55]. We then estimated GCI for multivariate series using the FIAR package[66] in R[55]. More specifically, we tested GCI of four multivariate series: (1) temperature (that is, mean annual temperature and temperature seasonality); (2) precipitation (that is, annual precipitation and precipitation seasonality); (3) land-use; and (4) temperature, precipitation, and land-use combined.

Methods references

48. Villaseñor, J. L. *El bosque húmedo de montaña en México y sus plantas vasculares: catálogo florístico-taxonómico*. (Comisión Nacional para el Conocimiento y Uso de la Biodiversidad - Universidad Nacional Autónoma de México, 2010).
49. POWO. Plants of the World Online. Facilitated by the Royal Botanic Gardens, Kew. Published on the Internet. (2019). Available at: http://www.plantsoftheworldonline.org. (Accessed: 24th September 2019)
50. GBIF. GBIF Occurrence Download. (2019). doi:https://doi.org/10.15468/dl.bdxzkw
51. Edwards, E. J., de Vos, J. M. & Donoghue, M. J. Doubtful pathways to cold tolerance in plants. *Nature* **521**, E5–E6 (2015).
52. Ramírez-Barahona, S., Sauquet, H. & Magallón, S. The delayed and geographically heterogeneous diversification of flowering plant families. *Nat. Ecol. Evol.* **4**, 1232–1238 (2020).
53. Carta, A., Peruzzi, L. & Ramírez-Barahona, S. A global phylogenetic regionalisation of vascular plants reveals a deep split between Gondwanan and Laurasian biotas. *bioRxiv* 1–15 (2021). doi:10.1101/2021.04.09.439199
54. Zizka, A. *et al.* CoordinateCleaner: Standardized cleaning of occurrence records from biological collection databases. *Methods Ecol. Evol.* **10**, 744–751 (2019).
55. R Core Team. R: A language and environment for statistical computing. *Vienna: R Foudation for Statistical Computing* (2020).
56. Brummitt, R. K. *World Geographic Scheme for Recording Plant Distributions, Edition 2*. (Hunt Institute for Botanical Documentation, Carnegie Mellon University, 2001).
57. Olson, D. M. *et al.* Terrestrial ecoregions of the world: a new map of life on Earth. *Bioscience* **51**, 933–938 (2001).
58. Kattge, J. *et al.* TRY - a global database of plant traits. *Glob. Chang. Biol.* **17**, 2905–2935 (2011).
59. Kattge, J., Bönisch, G. & Díaz, S, et al. TRY plant trait database – enhanced coverage and open access. *Glob. Chang. Biol.* **26**, 119–188 (2020).
60. Vale, M. M., Lima-ribeiro, M. S. & Rocha, T. C. Global land-use and land-cover data: historical, current and future secnarios. *Biodivers. Informatics* **16**, 28–38 (2021).
61. Karger, D. N. *et al.* Climatologies at high resolution for the earth's land surface areas. *Sci. Data* **4**, 170122 (2017).
62. Helwig, N. E. npreg: Nonparametric Regression via Smoothing Splines. R package version 1.0-6. (2021).
63. Bates, D., Martin, M., Bolker, B. & Walker, S. Fitting linear mixed-effects models using lme4. *J. Stat. Softw.* **67**, 1–48 (2015).
64. Hyndman, R. *et al.* forecast: forecasting functions for time series and linear

models. R package version 8.15. (2021).
65. Hyndman, R. & Khandakar, Y. Automatic time series forecasting: the forecast package for R. *J. Stat. Softw.* **26**, 1–22 (2008).
66. Roelstraete, B. & Rosseel, Y. FIAR: An R Package for Analyzing Functional Integration in the Brain. *J. Stat. Softw.* **44**, 1–32 (2011).

Acknowledgments

We are grateful to Jonás A. Aguirre Liguori for comments on earlier drafts. This work was supported by a CONACyT Ciencia de Frontera 2019 grant #263962 to S.R.-B.

Author contributions

S.R.-B. conceived the research with contributions from A.C.-R., K.F., J.F.O., and H.R.-C.; S.R.B. and A.C.-R compiled and curated the occurrence, climate, and land-use data; S.R.-B. designed and performed the analysis with contributions by K.F.; S.R.-B. wrote the manuscript with contributions with contributions from A.C.-R, K.F, A.E.O.-R., A.A.V.-A., J.F.O., and H.R.-C.

Competing interests

The authors declare no competing interests.

Data and code availability

The R code and data supporting the results in the main text are available at https://github.com/spiritu-santi/CF-mig and at Zenodo with the identifier https://doi.org/10.5281/zenodo.5587219. The geographic occurrence data is available through the Global Biodiversity Information Facility with the identifier https://doi.org/10.15468/dl.bdxzkw.

Additional information

Supplementary Information is available for this paper.

Correspondence and requests for materials should be addressed to Santiago Ramírez-Barahona.

Supplementary Files

This is a list of supplementary files associated with this preprint. Click to download.

- BMMSIfinal.pdf